minerals

MDPI

Article

Process Evaluation of an Iron Ore Operation Using the Floatability Component Model

Stefan Geldenhuys [1,*], Thiago Souza Pinto [2], Laurindo Leal Filho [3] and David Deglon [1]

[1] Centre for Minerals Research, Department of Chemical Engineering, University of Cape Town, Cape Town 7700, South Africa; david.deglon@uct.ac.za
[2] Centre of Mineral Development (CDM), Vale, Minas Gerais 33000-000, Brazil; thiago.souza@vale.com
[3] Mining and Petroleum Department, Polytechnic School, University of São Paulo, São Paulo 05508-010, Brazil; lauleal@usp.br
* Correspondence: stefan.geldenhuys@uct.ac.za

Abstract: The Brucutu iron ore mine (Minas Gerais, Brazil) is Vale's largest iron producing operation achieving around 21 million tons per annum. Evaluation of flotation performance is of high importance as even small gains can lead to large monetary benefits. Cell-by-cell samples of the froth products, selected feed and pulp-products were analyzed for flow rate, particle size distribution and chemical composition. In addition, certain samples were analyzed on an assay-by-size basis and hydrodynamic measurements of certain flotation cells were also performed. This detailed experimental dataset was then used to calibrate a floatability component model of the process. Longer mainline residence time resulted in significant Fe_2O_3 losses while yielding little benefit in terms of SiO_2 product grade. Scavenger 2 has twice the residence time of scavenger 1 while having to treat only 10% of the SiO_2, resulting in high Fe_2O_3 recoveries to the froth and poor separation. In addition, it is shown that the Fe_2O_3 exhibits true flotation behavior resulting in increased Fe_2O_3 losses. Simulations using the floatability component model identified avenues of process improvement to address the identified behavior. The insight provided by the simulations into the dynamics of the flotation process is invaluable for process engineers.

Keywords: froth flotation; process modeling; floatability component model; process improvement; metallurgical surveying

Citation: Geldenhuys, S.; Pinto, T.S.; Filho, L.L.; Deglon, D. Process Evaluation of an Iron Ore Operation Using the Floatability Component Model. *Minerals* **2021**, *11*, 589. https://doi.org/10.3390/min11060589

Academic Editors: Marisa Bezerra De Mello Monte, Iranildes Daniel dos Santos and Zhiyong Gao

Received: 11 May 2021
Accepted: 28 May 2021
Published: 31 May 2021

1. Introduction

Since its inception, froth flotation has undergone tremendous change as research tries to address the industrial challenges. The scale of flotation machines is ever changing from the 1 L batch flotation cell, that is the workhorse within many flotation laboratories, to large industrial mechanical cells, approaching volumes of 600 m^3. In addition, flotation technology is constantly evolving resulting in interesting new flotation machines. Research into the chemistry of froth flotation has also made large strides resulting in a plethora of collectors, depressants, frothers, etc. for the user to choose from. Within a constantly changing framework, industrial flotation engineers and operators need to achieve increasing throughputs and better product qualities, while struggling with ore variability and equipment maintenance. It is clear from this that applying a rigorous characterization of flotation circuits and determining optimization opportunities based on circuit models is vital to the success of an industrial operation.

Mineral recovery in froth flotation is generally accepted to follow first-order kinetics. Gorain [1] performed extensive research on the variation of the flotation rate within a variety of industrial flotation cells of different types and sizes, air rates, impeller speeds and froth depths. It was concluded that the differences in the rate constant seen within the

experimental program was due to a change in either ore floatability (P), bubble surface area flux (S_b), or the loss of recovery induced by the froth phase (R_f), as shown in Equation (1).

$$k = PS_bR_f \tag{1}$$

Substituting the rate constant into the recovery equation of a perfectly mixed reactor results in Equation (2), which predicts the recovery of floatable species, i.

$$R_i = \frac{PS_bR_f\tau}{1 + PS_bR_f\tau} \tag{2}$$

Within Equation (2), the bubble surface area flux (S_b) and residence time (τ) are based on known calculations that are quite simple to perform. That is, however, not the case for the ore floatability (P) and froth recovery (R_f). The ore floatability depends on numerous particle and mineral properties, such as but not limited to: particle size, degree of liberation, reagent coverage, mineral composition [2]. The complex behavior of an ore is often simplified by dividing the species into discrete floatability components, each assigned an average floatability (P) and a mass fraction (m_i) [3–6].

The definition of froth recovery (R_f) is the mass flow rate of particles recovered to the concentrate via selective bubble attachment over the mass flow rate of attached particles at the pulp froth interface [7,8]. Numerous attempts have been employed to physically measure the froth recovery with limited success [7–10]. For the reasons expressed above, ore floatability and froth recovery are usually fitted and therefore depend on the quality of the metallurgical and hydrodynamic survey.

Equation (2) deals with selective mineral recovery; however, within a separation process, non-selective entrainment of species is unavoidable. Recovery by entrainment (R_E) is known to be proportional to the amount of water recovered, as depicted by Equation (3) [11–15].

$$R_{E,\,i} = \frac{ENT_iR_w}{1 - R_w + ENT_iR_w} \tag{3}$$

If Equations (2) and (3) are combined, Equation (4) is obtained which provides a recovery equation incorporating selective and non-selective processes for a specific component, i [2,16,17].

$$R_i = \frac{PS_bR_f\tau(1 - R_w) + ENT_iR_w}{\left(1 + PS_bR_f\tau\right)(1 - R_w) + ENT_iR_w} \tag{4}$$

The prediction of recovery by entrainment relies solely on the water recovery, therefore a model predicting the water recovery is needed to capture the flotation performance. Water recovery was predicted by the relationship presented in Equation (5) [18].

$$Q_w = aQ_s^b \tag{5}$$

The aim of this paper is to use the data generated from a metallurgical survey conducted on the reverse flotation of iron ore in the "coarse" Brucutu circuit to calibrate the floatability component model. This model will then be used to assess the current behavior of the process and identify any optimization opportunities. Lastly, the calibrated model will be used to perform simulations focusing solely on circuit reconfiguration to maximize hematite grade and recoveries in the final concentrate. This study will provide unprecedented information and insight into the process behavior and will assist metallurgists with decision making.

2. Materials and Methods

This section will discuss the metallurgical sampling campaign performed at Vale's Brucutu operation to characterize the performance of the coarse iron ore reverse flotation circuit.

The coarse flotation circuit consists of 4 identical lines. Each line consists of two parallel lines (bank A and B) of 10 flotation cells which operate in rougher, cleaner and recleaner duties. The froth product from bank A and B is fed to a scavenging section consisting of 10 flotation cells in series. The first 5 flotation cells are referred to as Scavenger 1 whereas the last 5 flotation cells are referred to as Scavenger 2. The present work is related to a metallurgical survey campaign of the entire line 1 (including bank A and B and the scavenger cells) and a simplified flow diagram can be seen in Figure 1.

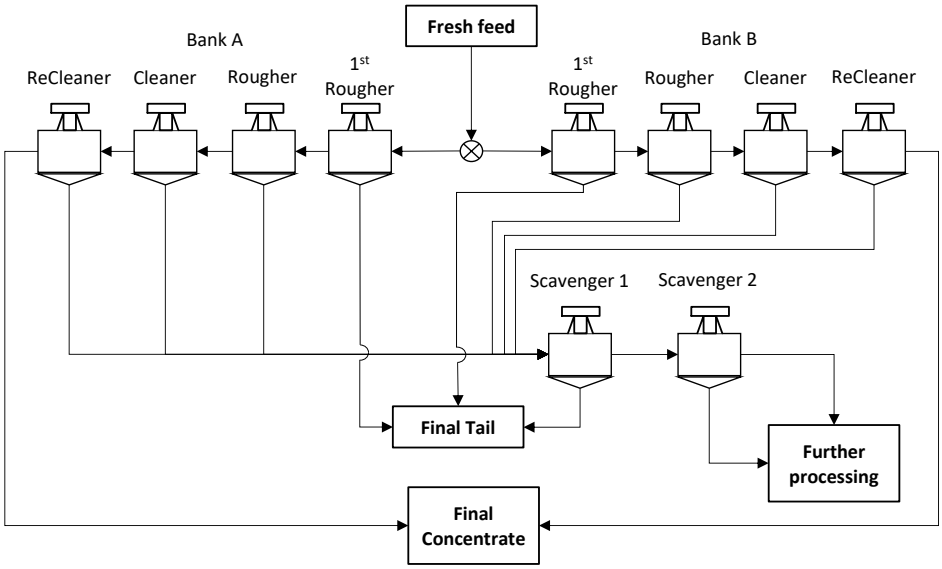

Figure 1. Diagram highlighting the process flow of line 1 coarse flotation at Brucutu.

2.1. Metallugical Characterization

2.1.1. Sampling Campaign

The metallurgical assessment was performed by sampling and performing the following measurements:

1. Cell-by-cell froth product flow rate, chemical analysis, and particle size distribution;
2. Selected (based on sampling access) feed and pulp product chemical analysis and particle size distribution;
3. Bank-by-bank froth product as well as selected feed and pulp product chemical analysis by size.

It should be noted that the entire sampling campaign was performed over a period of one week.

2.1.2. Hot Flotation Tests

Hot batch flotation tests were performed on the composite tailing streams from the bank B rougher, cleaners, and recleaners as well as the concentrate streams from the scavenger 1 and 2 banks. The tests were performed in 2.5 L Denver batch flotation cell. Five froth products were collected at time intervals of 20, 40, 60, 120, and 180 s.

2.1.3. Sample Analysis

The elements analyzed for (unsized and sized) are Fe, SiO_2, P, Al_2O_3, Mn, TiO_2, CaO and MgO. All samples were sized (including the assay-by-size samples) into the following size fractions: +250 μm, +150 μm, +106 μm, +75 μm, +45 μm, and −45 μm. It should be

noted that due to sample mass constraints the hot batch flotation tests were only assayed on an unsized basis.

2.2. Hydrodynamic Characterization

To simplify the experimental campaign, hydrodynamic measurements were taken at a single fixed point (depending on access) for all the flotation cells. The superficial gas velocity (J_g) and bubble diameter (d_b) were measured using the Anglo American Platinum Bubble Sizer (APBS) (Stone Three, Cape Town, South Africa). The gas hold-up (ε_g) was measured using a methodology similar to Power [19] however the probe used mechanically activated valves instead of pneumatic pinch valves. It should be noted the hydrodynamic measurements on cell 3 to 5 of Scavenger 1 were abandoned due to safety concerns.

2.3. Modeling and Simulation

Model fitting of parameters such as the ore floatability and froth recovery was performed in Microsoft Excel. To simplify the modeling methodology, it was decided that only Fe_2O_3 and SiO_2 would be modeled separately whereas the remaining elements are all grouped together as remainder. Simulations were conducted in JKSimFloat (v6.1, JKTech, Brisbane, Australia).

3. Results

This section will present and discuss the results from the survey campaign and simulation scenarios regarding Fe_2O_3 and SiO_2 only. This will be divided into three main sections, namely: gas dispersion, metallurgical performance, and simulation scenarios.

3.1. Gas Dispersion

The coarse flotation circuit consists of dated Wemco #164 and #144 flotation cells with self-aerating mechanisms. The air flow induced is mostly a function of impeller speed and, therefore, hydrodynamic measurements are very important as they provide an indication of mechanism wear. These measurements are usually neglected within self-aerated cells leading to poor dispersion as well as poor detection and/or maintenance planning. Figure 2 displays the measured bubble size and gas hold-up as a function of the measured superficial gas velocity.

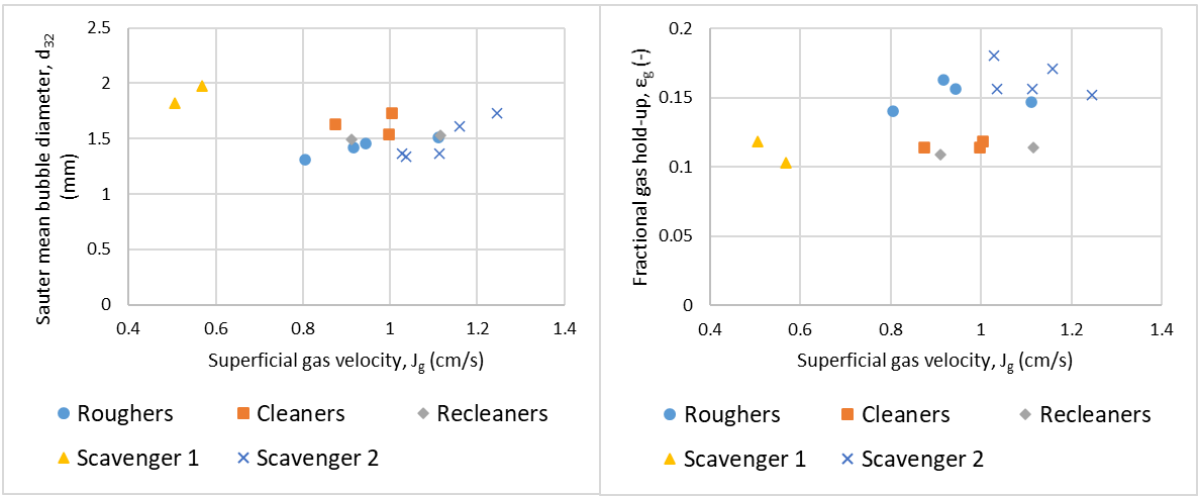

(**a**) (**b**)

Figure 2. Hydrodynamic measurements for bank B represented as (**a**) Sauter mean bubble diameter as a function of superficial gas velocity, and (**b**) fractional gas hold-up as a function of superficial gas velocity.

Figure 2a indicates that the superficial gas velocities ranged between 0.8 cm/s and 1.2 cm/s which is within the expected range [19–21] apart from Scavenger 1 cell 1 and 2 which operated at ± 0.5 cm/s; this can be considered as low. The Sauter mean bubble diameter (d_{32}) ranged from 1 mm to 2 mm which is within the expected range [19–21]. For the most part, all measurements fall onto a common linear operating line where an increase in superficial gas velocity results in an increase in bubble size. As noted before, cell 1 and 2 of Scavenger 1 significantly deviates from the observed trend and this is possibly an indication of a faulty and/or wore out mechanism. Figure 2b indicates that the measured gas hold-up ranged between 10% and 20% which is within what one would normally expect [19–21].

3.2. Metallurgical Performance

3.2.1. Fe_2O_3 and SiO_2 Behavior

The main objective within an iron ore flotation circuit is to depress the hematite (Fe_2O_3) while selectively recovering the quartz (SiO_2), in a reverse flotation operation. Figure 3 highlights the relation between size and recovery for both Fe_2O_3 and SiO_2 and this is fundamental to the performance of an iron ore operation as it highlights the relative floatability of both hematite and quartz. The induced selectivity can be seen in Figure 3, as the hematite recovery-by-size is much lower than the quartz recovery-by-size, therefore allowing an effective split. Figure 3a highlights that the recovery of quartz follows the classical n-shaped recovery behavior, typical of a floating species, i.e., a drop-off in fine recovery due to poor collision efficiency and a drop-off in coarse recovery due high probabilities of detachment [22–24]. It is important to note that the relative performance for 1A Ro1 highlights lower recoveries since it is a single flotation cell. Characterization of the 1A Ro1 performance is very important to the operation, as the tail produced by the flotation cell reports directly to final tail.

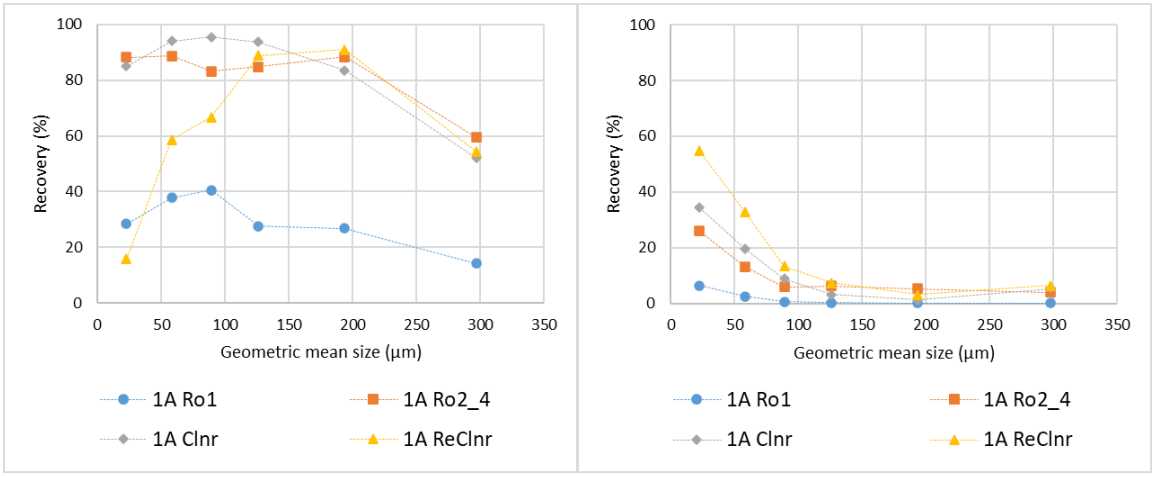

(**a**) (**b**)

Figure 3. Recovery-by-size of line 1 bank A for (**a**) SiO_2, and (**b**) Fe_2O_3 (1A refers to line 1 bank A, Ro refers to rougher, Clnr refers to cleaner, and ReClnr refers to recleaner).

The hematite behavior reported in Figure 3b is much more complicated. To aid the discussion, the data will be discussed based on particles being larger or smaller than 50 µm. This size (50 µm) is important as it has been highlighted by many researchers as the size at which entrainment becomes insignificant [13,25,26].

If the behavior of particles larger than 50 µm is observed in Figure 3b, it can be seen that there is still significant recovery in these size classes which is unexpected for a specie recovered by non-selective entrainment only. It is thought that this phenomenon can be explained by the presence of composite particles of quartz and hematite (poor liberation) within the coarser size fractions [15].

The focus is now shifted to particles smaller than 50 µm with special emphasis on the sub 45 µm size fraction. It is commonly accepted that recovery by entrainment will exhibit a linear relationship with water recovery, as first proposed by Lynch [11]. Due to the classification of solids with respect to water in both the pulp and froth phases, this relationship is expected to be less than 1:1, the slope being related to the entrainability (ENT) factor. For the measured −45 µm hematite recovery, this relationship was not observed, and many of the experimental points showed hematite mass recovery being higher than that of water as shown in Figure 4.

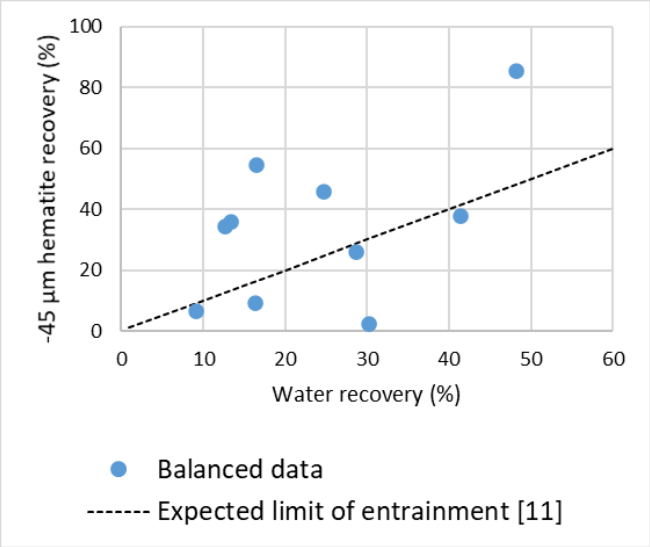

Figure 4. −45 µm hematite recovery as a function of measured water recovery.

In a similar plot to Figure 4, Lima [15] demonstrated that sub 38 µm Fe-bearing mineral recovery never exceeded that of water. Most hematite particles are liberated at a relatively coarse size, around 100 µm, and therefore, poor liberation is not a plausible explanation of why particles of sub 45 µm did not follow the measured water recovery. Since this observation was made, further investigations by Vale into this phenomenon has attributed this to short residence times within the starch conditioning tanks. This leads to the hematite experiencing true flotation mainly by electrostatic interaction with the amine collector. This is a significant conclusion and highlights the importance of performing metallurgical characterizations of the circuit within a reasonable frequency.

3.2.2. Circuit Performance

The observations regarding the overall circuit performance can be divided into three basic themes, namely: bank A and B rougher 1 tail, mainline residence time, and scavenger residence time. In the current circuit configuration, the froth product from the 1st rougher of each bank reports to the final tail. Based on the plant feed, the hematite recovery is 2.7% and 4.8% for the first rougher cell of bank A and B, respectively. Expressed in this manner, these hematite losses seem quite reasonable. However, as illustrated in Figure 5, based on the distribution in the final tail with regards to where it originates from, nearly 36% of the hematite losses in the final tail originates from the first rougher tail of bank A and B.

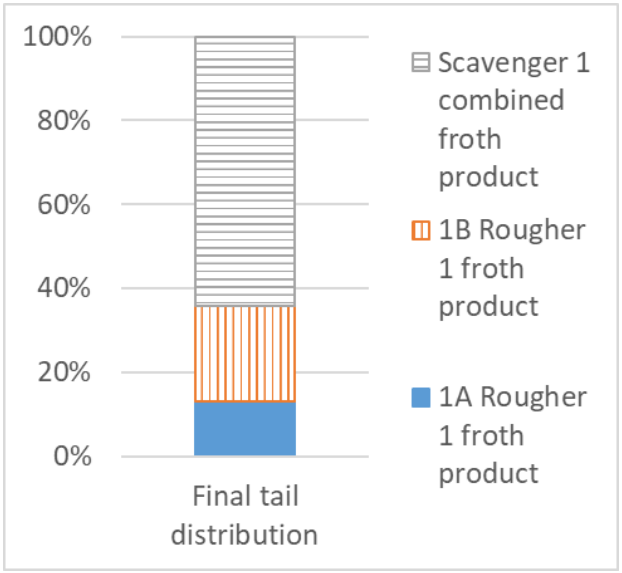

Figure 5. Distribution of hematite in line 1 final tail based on where it originates from.

Figure 6 displays the recovery/time plots for the flotation banks.

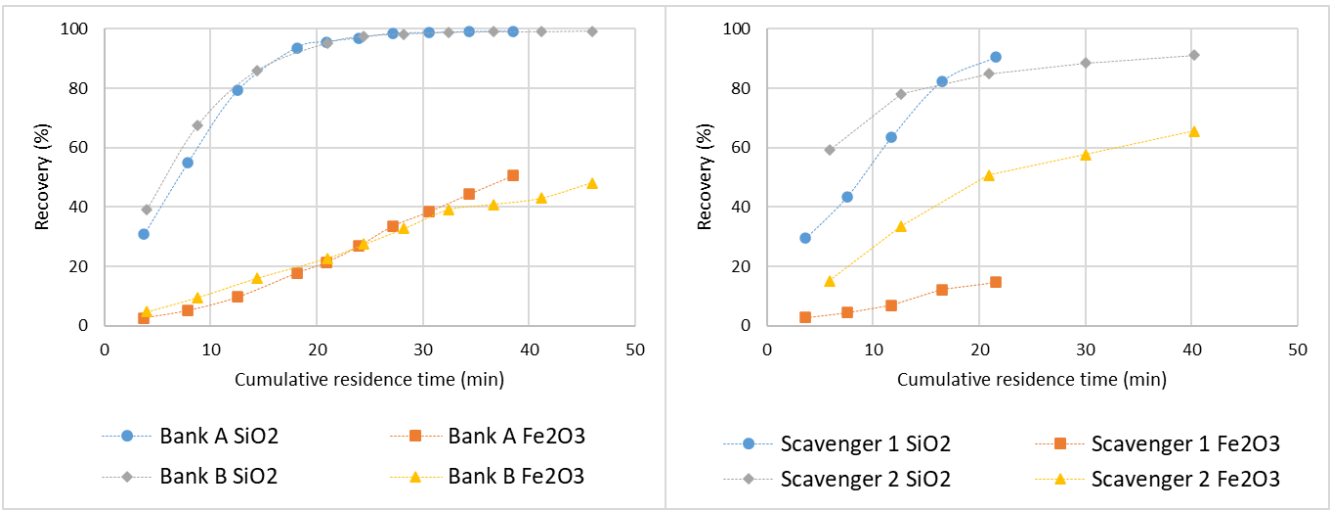

(**a**) (**b**)

Figure 6. Hematite and quartz recovery as a function of the cumulative bank residence time for (**a**) roughers, cleaners, and recleaners of bank A and B, and (**b**) scavenger 1 and 2.

Figure 6a suggests that the residence time in the mainline (where mainline refers to the roughers, cleaners, and recleaners) is around 38 min and 45 min for bank A and B, respectively. A long residence time within the mainline is beneficial for quartz recovery, which is an important driver, but it is also results in more hematite losses to the froth. It can be seen from Figure 6a that the quartz recovery plateaus at a residence time of ±25 min. The remaining flotation time (25 min to 40 min) has virtually no effect on the quartz recovery but drastically increases the amount of hematite recovered to the froth product. This highlights the importance of residence time of the mainline within an iron ore operation. The reasoning behind having a long residence time to obtain SiO_2 grades lower than 1 wt% in the final concentrate, thus producing a premium product that ultimately sells for a higher price, is valid. However, this is usually accompanied by higher hematite losses. This trade-off is of critical importance within the circuit.

Figure 6b highlights that the residence time of scavenger 2 is nearly twice that of scavenger 1 (21 min compared to 40 min). The short residence time within scavenger 1 is beneficial as it allows the process to exploit the floatability differences of quartz and hematite. Scavenger 1 recovers nearly 90% of the quartz fed to it which leaves a small fraction of quartz left to be recovered by scavenger 2, even though, it has a much longer residence time. The benefit of the short residence time in scavenger 1 can be seen as this bank only recovers 15% of the hematite fed to it whereas scavenger 2 recovers nearly 60%. As mentioned previously, residence time is an important parameter that should be used to exploit the relative differences in the kinetics of quartz and hematite, and this carries through to the scavenger circuit. The relatively short residence time of scavenger 1 still recovers most of the quartz (90%) while minimizing hematite losses to only 15%.

3.3. Simulation Results

As demonstrated by Figure 5, the hematite losses that can be contributed to the rougher 1 tail of bank A and B is around 36% of the total hematite lost to the final tail. Aiming at decreasing these hematite losses, scenario 1 will evaluate the value of rerouting the rougher 1 tail from both bank A and B to the feed of scavenger 1. Figure 7 indicates that, by rerouting the rougher 1 tail of both bank A and B to the feed of the scavengers, a significant decrease in hematite losses to the final tail can be realized. The recovery of hematite to the final tail decreases from 14.8% to 10.5% indicating a recovery gain of around 4%. This is further illustrated by the drop of hematite grade within the final tail by nearly 4.5 wt%. It should be noted that this does decrease the scavenger 1 residence time, and therefore, the quartz recovery in this bank drops from 84% to 79%. However, the excess residence time available in scavenger 2 will ensure that the quartz recovery over both scavenger banks remains constant.

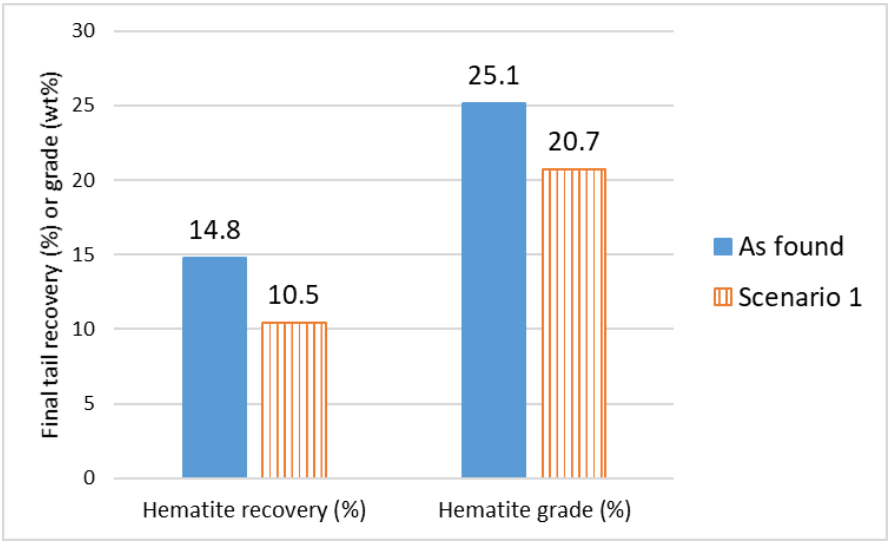

Figure 7. Final tail hematite recovery based on plant feed and grade for "as found" and scenario 1.

In the current circuit configuration, the scavenger 2 concentrate forms part of the feed to a subsequent concentrating step. The long residence time of the scavenger 2 bank has been mentioned a few times; however, due to this, it produces a concentrate containing 98.6 wt% hematite and 1.0 wt% quartz (virtually the final concentrate quality). This leads to the scenario 2 simulation which has an option A and B. Option A reroutes the scavenger 2 concentrate to a final concentrate because the chemical analysis indicated that no further processing is needed. Option B reroutes the scavenger 2 concentrate to the feed of the mainline to address the residence time concerns in the mainline highlighted previously. The results of these simulations are shown in Figure 8.

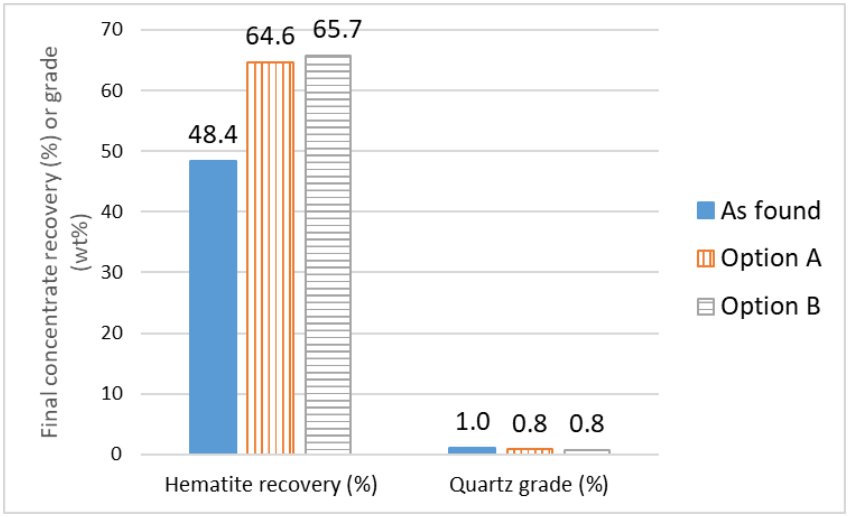

Figure 8. Final concentrate hematite recovery, based on plant feed, and quartz grade for "as found" and option A and B of scenario 2.

It comes as no surprise that the hematite recovery increased significantly as the hematite within the scavenger 2 concentrate is now reporting to the final concentrate of line 1. It is important to note that the selling price of the final product is very dependent on the quartz grade, and therefore, it makes sense that the operation is conservative in defining its operating strategy. However, due to the long residence time within scavenger 2, adding this stream to the final concentrate poses no risk and significantly increases the hematite recovery. Interestingly, option B, which is recycling this stream to the feed of the plant, shows marginally better performance compared to option A. Initially, this might not make sense; however, this a result of managing the mainline residence time. Shorter residence times, which is what the addition of this stream to plant feed is causing, allows one to efficiently exploit the difference in hematite and quartz floatability resulting in an overall better split in the mainline. The volume of this stream is relatively small, and therefore, the resultant benefit is also small; however, it does highlight the importance of this concept. Scenario 3 will explore this idea in more detail.

It should be noted that the simulations performed within scenario 3 are done solely to explore the concept of excess scavenger and mainline residence time. The calibrated FCM relies on many assumptions, for instance, constant froth recovery, and therefore will not reflect the actual process performance. However, perfectly predicting the process behavior is not necessarily the point of using the FCM, rather it gives engineers a means to test hypotheses. If these prove to be significant in the simulator, a rigorous testing campaign should be used to validate the behavior of the process. Figure 9 displays the simulation results of shortening the scavenger bank residence time. This was done by reducing the number of scavenger cells that are online. The important output variables are the quartz grade and hematite recovery to the final concentrate as well as the volumetric flow rate of the recirculating stream.

Figure 9a highlights the increasing volumetric flow rate of the recirculating stream (scavenger concentrate) as the overall scavenger residence time is decreased. This increases the volumetric feed to the mainline which leads to a decrease in the residence time within the mainline. The resulting improvement in quartz and hematite behavior is seen in Figure 9b. This improvement is a direct result of a more efficient separation within the mainline, i.e., shorter residence times reduce the entrainment of hematite to the froth while the quartz recovery remains unaffected. This clearly illustrates the benefit of operating with a recycle within an iron ore flotation circuit; however, it should be noted that there are process concerns. Firstly, if the scavenger residence time is too short, the process will be difficult to control. Due to the exponential response in the volumetric flow of the recycle even small process changes (increases in throughput is one example) can drastically affect

this stream and subsequently the volume balance across the process. Secondly, the recycle stream is dependent on the quality of the ore fed to the plant and significant changes in the quartz feed grade (for instance) coupled with a scavenger residence time that is too short will result in a large change in the volume of the recycle stream, thus affecting process stability and control. To mitigate these risks, most iron ore flotation circuits are designed with excess scavenger residence time which can counteract the benefits of running a recycle while adding unnecessary process complexity. This illustrates the benefit of this work, as it significantly contributes to the collaboration between engineers and operators while also aiding the understanding of this relationship.

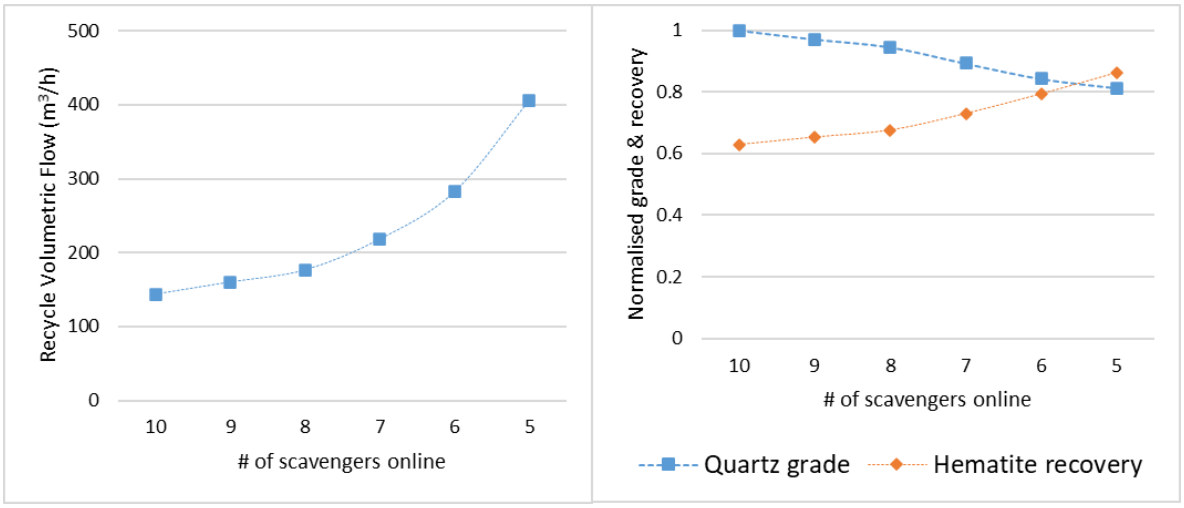

(**a**) (**b**)

Figure 9. Scenario 3 simulation results highlighting (**a**) the recirculating volumetric flow rate, and (**b**) the normalized quartz grade and hematite recovery of the final concentrate both as a function of the number of online scavenger cells.

4. Conclusions

An extensive survey was conducted on an iron ore reverse flotation circuit operating with dated Wemco flotation cells. The data from the survey were used to calibrate a floatability component model (FCM). The survey results indicated that there may be potential to improve the circuit performance by adjusting the circuit residence times. Simulations were performed of various circuit configurations. Re-routing the rougher 1 froth product of both bank A and B from the final tail to the scavenger feed was shown to result in less hematite losses to the final tail. It was also shown that there were benefits associated with diverting the scavenger 2 pulp product to a final concentrate, as it is already of final concentrate quality and further processing could incur unnecessary losses. The importance of managing the mainline and scavenger residence time was illustrated by simulations focusing on decreasing the scavenger residence time and recycling the scavenger pulp product to the feed of the flotation circuit. These are powerful insights and demonstrate how the FCM, which is a very simplified model of flotation, helps guide the operators and metallurgists on how to improve the process by enabling interrogation at a level not previously possible.

Author Contributions: Conceptualization, S.G., T.S.P., L.L.F. and D.D.; methodology, S.G., T.S.P., L.L.F. and D.D.; project administration, S.G., T.S.P., L.L.F. and D.D.; funding acquisition, S.G., T.S.P., L.L.F. and D.D.; data acquisition, T.S.P.; data analysis, S.G. and T.S.P.; writing—original draft preparation, S.G. and T.S.P.; writing—review and editing, S.G., T.S.P., L.L.F. and D.D. All authors have read and agreed to the published version of the manuscript.

Funding: This research was funded by Vale S.A.

Data Availability Statement: Data sharing is not applicable.

Acknowledgments: The authors would like to thank the Vale S.A., CDM, CNPq and Brucutu site personnel for the support and assistance along this work.

Conflicts of Interest: The authors declare no conflict of interest.

References

1. Gorain, B.K.; Napier-Munn, T.J.; Franzidis, J.P.; Manlapig, E.V. Studies on impeller type, impeller speed and air flow rate in an industrial scale flotation cell. Part 5: Validation of the k-Sb relationship and effect of froth depth. *Miner. Eng.* **1998**, *11*, 615–626. [CrossRef]
2. Welsby, S.D.D.; Vianna, S.M.S.M.; Franzidis, J.P. Assigning physical significance to floatability components. *Int. J. Miner. Process.* **2010**, *97*, 59–67. [CrossRef]
3. Kelsall, D.F. Application of probability in the assessment of flotation systems. *Trans. Inst. Min. Metall.* **1961**, *70*, 191–204.
4. Imaizumi, T.; Inoue, T. Kinetic considerations of froth flotation. In Proceedings of the 6th International Mineral Processing Congress, Cannes, France, 26 May–2 June 1963; pp. 581–593.
5. Runge, K.C.; Harris, M.C.; Frew, J.A.; Manlapig, E.V. Floatability of stream around the Cominco Red Dog lead cleaning circuit. In Proceedings of the 6th Mill Operators Conference, Madang, Papua New Guinea, 6–8 October 1997; AusIMM: Melbourne, Australia, 1997; pp. 157–163.
6. Runge, K.C.; Franzidis, J.P.; Manlapig, E.V. Structuring a flotation model for robust prediction of flotation circuit performance. In Proceedings of the XXII International Mineral Processing Congress, Cape Town, South Africa, 29 September–3 October 2003; Lorenzen, L., Bradshaw, D.J., Eds.; SAIMM: Marshalltown, South Africa, 2003; pp. 973–984.
7. Savassi, O.N.; Alexander, D.J.; Johnson, N.W.; Manlapig, E.V.; Franzidis, J.P. Measurement of froth recovery of attached particles in industrial cells. In Proceedings of the Sixth Mill Operators Conference, Madang, Papua New Guinea, 6–8 October 1997; pp. 149–155.
8. Vera, M.A.; Franzidis, J.P.; Manlapig, E.V. Simultaneous determination of collection zone rate constant and froth zone recovery in a mechanical flotation environment. *Miner. Eng.* **1999**, *12*, 1163–1176. [CrossRef]
9. Alexander, D.J.; Franzidis, J.P.; Manlapig, E.V. Froth recovery measurement in plant scale flotation cells. *Miner. Eng.* **2003**, *16*, 1197–1203. [CrossRef]
10. Seaman, D.R.; Franzidis, J.P.; Manlapig, E.V. Bubble load measurement in the pulp zone of industrial flotation machines—A new device for determining the froth recovery of attached particles. *Int. J. Miner. Process.* **2004**, *74*, 1–13. [CrossRef]
11. Lynch, A.J.; Elber, L. Modelling and Control of Mineral Processing Plants. *IFAC Proc. Vol.* **1980**, *13*, 25–32. [CrossRef]
12. Trahar, W.J. A rational interpretation of the role of particle size in flotation. *Int. J. Miner. Process.* **1981**, *8*, 289–327. [CrossRef]
13. Smith, P.G.; Warren, L.J. Entrainment of particles into flotation froths. *Miner. Process. Extr. Metall. Rev.* **1989**, *5*, 123–145. [CrossRef]
14. Zheng, X.; Johnson, N.W.; Franzidis, J.P. Modelling of entrainment in industrial flotation cells: Water recovery and degree of entrainment. *Miner. Eng.* **2006**, *19*, 1191–1203. [CrossRef]
15. Lima, N.P.; de Souza Pinto, T.C.; Tavares, A.C.; Sweet, J. The entrainment effect on the performance of iron ore reverse flotation. *Miner. Eng.* **2016**, *96*, 53–58. [CrossRef]
16. Savassi, O.N. Direct Estimation of the Degree of Entrainment and the Froth Recovery of Attached Particles in Industrial Flotation Cells. Ph.D. Thesis, University of Queensland, Brisbane, Australia, 1998.
17. Harris, T.A. The Development of a Flotation Simulation Methodology towards an Optimisation Study of UG2 Platinum Flotation Circuit. Ph.D. Thesis, University of Cape Town, Cape Town, South African, 2000.
18. Alford, R.A. Improved model for design of industrial column flotation circuits in sulphide applications. In *Sulphide Deposits—Their Origin and Processing*; Springer: Dordrecht, The Netherlands, 1990; pp. 189–206.
19. Power, A.; Franzidis, J.P.; Manlapig, E.V. The characterisation of hydrodynamic conditions in industrial flotation cells. In Proceedings of the Seventh Mill Operators Conference, Kalgoorlie, Australia, 12–14 October 2000; AusImm: Melbourne, Australia, 2000; pp. 243–253.
20. Deglon, D.A.; Egya-Mensah, D.; Franzidis, J.P. Review of hydrodynamics and gas dispersion in flotation cells on South African platinum concentrators. *Miner. Eng.* **2000**, *13*, 235–244. [CrossRef]
21. Malinga, T.; Turrer, H.; Nascimento, C.; Russo, J.; Silva, J.; Gonzaga, F.; Machado, L.; Sweet, J. Gas Dispersion Measurements as a Diagnostic Tool for the Performance of Industrial Flotation Cells At Minas-Rio. In Proceedings of the Ironmaking, Iron Ore and Agglomeration Seminars, Sao Paulo, Brazil, 2–4 October 2018; ABM: Sao Paulo, Spain, 2018; pp. 296–307. [CrossRef]
22. Crawford, R.; Ralston, J.R. The influence of particle size and contact angle in mineral flotation. *Int. J. Miner. Process.* **1988**, *23*, 1–24. [CrossRef]
23. Ahmed, N.; Jameson, G.J. Flotation Kinetics. *Miner. Process. Extr. Metall. Rev.* **1989**, *5*, 77–99. [CrossRef]
24. Safari, M.; Harris, M.; Deglon, D.; Filho, L.L.; Testa, F. The effect of energy input on flotation kinetics. *Int. J. Miner. Process.* **2016**, *156*, 108–115. [CrossRef]
25. Savassi, O.N.; Alexander, D.J.; Franzidis, J.P.; Manlapig, E.V. An empirical model for entrainment in industrial flotation plants. *Miner. Eng.* **1998**, *11*, 243–256. [CrossRef]
26. Wiese, J.G.; O'Connor, C.T. An investigation into the relative role of particle size, particle shape and froth behaviour on entrainment of chromite. *Int. J. Miner. Process.* **2016**, *156*, 127–133. [CrossRef]